Acta Crystallographica Section F
Structural Biology and Crystallization Communications
ISSN 1744-3091

Crystallization and preliminary crystallographic analysis of *Arabidopsis thaliana* EDS1, a key component of plant immunity, in complex with its signalling partner SAG101

Stephan Wagner,[a]‡ Steffen Rietz,[b]‡ Jane E. Parker[b]* and Karsten Niefind[a]*

[a]Institute for Biochemistry, University of Cologne, Zülpicher Str. 47, D-50674 Köln, Germany, and [b]Department of Plant–Microbe Interactions, Max Planck Institute for Plant Breeding Research, Carl-von-Linné Weg 10, D-50829 Köln, Germany

‡ These authors should be considered joint first authors.

Correspondence e-mail: parker@mpipz.mpg.de, karsten.niefind@uni-koeln.de

Received 24 November 2010
Accepted 6 December 2010

In plants, the nucleocytoplasmic protein EDS1 (Enhanced disease susceptibility1) is an important regulator of innate immunity, coordinating host-cell defence and cell-death programs in response to pathogen attack. *Arabidopsis thaliana* EDS1 stabilizes and signals together with its partners PAD4 (Phytoalexin deficient4) and SAG101 (Senescence-associated gene101). Characterization of EDS1 molecular configurations *in vitro* and *in vivo* points to the formation of structurally and spatially distinct EDS1 homomeric dimers and EDS1 heteromeric complexes with either PAD4 or SAG101 as necessary components of the immune response. EDS1, PAD4 and SAG101 constitute a plant-specific protein family with a unique 'EP' (EDS1–PAD4-specific) domain at their C-termini and an N-terminal domain resembling enzymes with an α/β-hydrolase fold. Here, the expression, purification and crystallization of a functional EDS1 complex formed by EDS1 and SAG101 from *Arabidopsis thaliana* are reported. The crystals belonged to the orthorhombic space group $P2_12_12_1$, with unit-cell parameters $a = 101.8$, $b = 115.9$, $c = 122.8$ Å, and diffracted to 3.5 Å resolution.

1. Introduction

The plant innate immune system relies on tight regulation of defence and cell-death programs triggered in individual cells by an attacking pathogen. In the model plant *Arabidopsis thaliana*, EDS1 (Enhanced disease susceptibility1; Aarts *et al.*, 1998; Falk *et al.*, 1999) has emerged as a central immune regulator (Wiermer *et al.*, 2005; García & Parker, 2010). Together with its sequence-related partners PAD4 (Phytoalexin deficient4) and SAG101 (Senescence-associated gene101), EDS1 controls low-level 'basal' immunity to virulent pathogens and a more acute resistance reaction involving programmed cell death mediated by certain intracellular nucleotide-binding leucine-rich repeat (NB-LRR) receptors that recognize specific pathogen effectors (Zhou *et al.*, 1998; Jirage *et al.*, 1999; Feys *et al.*, 2001, 2005).

Arabidopsis EDS1 is a soluble nucleocytoplasmic protein that forms molecularly and spatially different complexes with PAD4 and SAG101 *in vivo* (Feys *et al.*, 2005). Analysis of the molecular configurations of individual EDS1 complexes expressed in yeast or as recombinant proteins purified from *Escherichia coli* showed that EDS1 can form homomeric dimers and stabilize PAD4 and SAG101 in heteromeric associations (S. Rietz & J. Parker, unpublished results). The data indicate that EDS1 uses different structural determinants to interact with PAD4 or SAG101 in separate complexes that have different signalling activities. Whereas EDS1 dimers are mostly cytoplasmic *in vivo*, EDS1–PAD4 heteromeric complexes accumulate in the nucleus and cytoplasm and EDS1–SAG101 complexes are confined to nuclei (Feys *et al.*, 2005). The presence of distinct EDS1 complexes in different cellular compartments suggests that dynamic interactions between EDS1 nuclear and cytoplasmic pools are important in defence signal relaying. Indeed, coordination between the EDS1 cytoplasmic and nuclear pools *via* the nuclear pore trafficking machinery is necessary for resistance to pathogens (Cheng *et al.*, 2009; García *et al.*, 2010).

Based on primary-sequence analysis, the N-terminal domain of EDS1 has homology to proteins of the α/β-hydrolase fold family, including three residues that comprise a serine hydrolase Ser-Asp-His catalytic triad (Ollis *et al.*, 1992). EDS1 shares this overall homology and a unique C-terminal 'EP' (EDS1–PAD4-specific) domain with PAD4 and SAG101, although SAG101 lacks the canonical catalytic triad (He & Gan, 2002; Wiermer *et al.*, 2005). While low acyl esterase activity was found for SAG101 (He & Gan, 2002), neither EDS1 nor PAD4 has been reported to possess serine esterase catalytic activity. However, EDS1 and PAD4 are needed to transduce reactive-oxygen-species-derived signals leading to cell death in photooxidative stress and immune responses, suggesting the involvement of a redox component in EDS1 signal transduction (Mateo *et al.*, 2004; Mühlenbock *et al.*, 2008; Straus *et al.*, 2010).

The combined genetic and molecular data position EDS1 as a central biotic stress signalling 'node' in plants, but a detailed biochemical mechanism for the coordination of multiple defence outputs by EDS1 remains elusive. To investigate the physicochemical nature of the associations and functional dynamics of EDS1, we undertook the purification of EDS1 complexes from *E. coli* for crystallization. Here, we report the expression, purification and crystallization of an *A. thaliana* EDS1–SAG101 heterodimer. Structure solution of this complex should provide crucial mechanistic insights into the pathways operating in plant innate immunity.

2. Materials and methods

2.1. Protein expression and purification

The EDS1 coding sequence (Falk *et al.*, 1999) was amplified by PCR using oligonucleotides containing *Nde*I/*Xho*I restriction sites and was cloned into pET42a(+) (Invitrogen) without an additional tag. The SAG101 coding sequence (Feys *et al.*, 2005) was amplified as a *Bam*HI/*Kpn*I fragment and was cloned into pRSF-Duet (Invitrogen) as an N-terminal His-tag fusion. Both constructs were subsequently transformed separately into *E. coli* strain BL21 (DE3) Rosetta (Novagen). Expression of a 0.4 l culture in LB medium was induced at an OD of 0.8 with 0.2 m*M* IPTG and the cells were shaken at 180 rev min^{-1} overnight at 285 K.

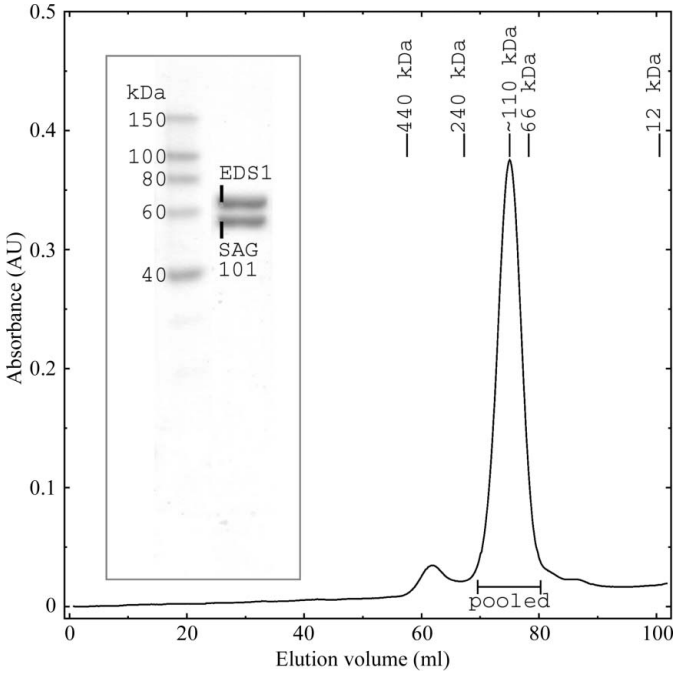

Figure 1
Size-exclusion chromatogram and SDS–PAGE analysis of the EDS1–SAG101 heterodimer. The retention volumes of four standard proteins (ferritin, 440 kDa; catalase, 240 kDa; bovine serum albumin, 66 kDa; RNase, 12 kDa) are shown as references. The major peak at a volume of 75.01 ml corresponds to a calculated mass of approximately 110 kDa and was analyzed by denaturing SDS–PAGE. The indicated fractions were pooled and used for subsequent experiments.

The cells were harvested by centrifugation and resuspended in buffer *A* (50 m*M* NaH_2PO_4, 100 m*M* NaCl, 20 m*M* imidazole, 1 m*M* DTT, 10% glycerol pH 8.0) with 1 mg ml^{-1} lysozyme and 10 µg ml^{-1} DNase I. Cells expressing EDS1 and His-SAG101 were mixed at this stage to allow the binding of nontagged EDS1 to His-SAG101. After 30 min incubation on ice, the cells were sonicated for a total of 2 min (four cycles, 40% output). Cell debris was removed by centrifugation at 20 000*g* for 30 min at 277 K. The supernatant was filtered and loaded onto a 1 ml Ni–NTA Superflow column (Qiagen) pre-equilibrated with buffer *A*. After rigorous washing (ten column volumes) with buffer *A*, the complex was eluted in a buffer consisting of 50 m*M* NaH_2PO_4, 100 m*M* NaCl, 250 m*M* imidazole, 1 m*M* DTT, 10% glycerol pH 7.5. The eluate was concentrated to a volume of less than 1.5 ml, applied onto a HiLoad 16/60 Superdex 200 size-exclusion column (Amersham Pharmacia) and eluted in 40 m*M* imidazole, 50 m*M* NaCl, 1 m*M* DTT pH 7.4.

The purity and stoichiometry of the complex were checked by SDS–PAGE analysis. Fractions containing pure complex were pooled and concentrated to 8–12 mg ml^{-1} using Amicon-15 ultrafiltration units (Millipore).

2.2. Crystallization

All crystallization experiments were performed at 293 K using the sitting-drop vapour-diffusion method. Initial screens were set up in 96-well plates (Art Robbins) using commercial sparse-matrix and grid screens from Hampton Research and Jena Bioscience. The crystallization drops were pipetted with a nanolitre dispenser (Hydra II, Matrix Technologies) and 400 nl protein solution was mixed with 400 nl reservoir solution. An initial crystallization condition [100 m*M* HEPES, 10%(*w*/*v*) PEG 4000, 5%(*v*/*v*) 2-propanol pH 7.5] was optimized in a Cryschem 24-well plate by mixing 1 µl protein solution with 1 µl reservoir solution, varying the pH value and precipitant concentration.

2.3. Data collection and analysis

Prior to data collection, crystals were cryoprotected by transferring them stepwise into a stabilizing solution [100 m*M* HEPES, 12%(*w*/*v*) PEG 4000, 5%(*v*/*v*) 2-propanol pH 7.3] containing increasing concentrations of glucose [starting at 5%(*w*/*v*) and increasing after 2 min incubation at each step to a final concentration of 35%(*w*/*v*)]. The crystals were mounted in a nylon loop and flash-frozen in a 100 K nitrogen stream. Diffraction data were collected on beamline 14.2 at BESSY (Berlin) equipped with a MAR 224 CCD detector. The raw diffraction data were integrated with *XDS* (Kabsch, 2010) and scaled with *SCALA* (Collaborative Computational Project, Number 4, 1994).

3. Results and discussion

We were able to express and purify recombinant EDS1 protein in complex with SAG101 derived from *A. thaliana*. During preparative size-exclusion chromatography, the complex eluted with a retention volume that corresponded to a molecular mass of approximately 110 kDa. Considering the limited accuracy of mass determination by

gel filtration, this result is broadly consistent with a heterodimer of EDS1 (71.6 kDa) and SAG101 (62.1 kDa) (Fig. 1). Moreover, SDS–PAGE analysis unambiguously showed that an EDS1–SAG101 heterodimer and not an EDS1 homodimer was purified (Fig. 1).

Crystallization trials using various commercial screens produced one initial hit for EDS1–SAG101 crystals, the identity of which we verified by mass spectrometry. The optimized crystals grew using 100 m*M* HEPES, 10%(*w*/*v*) PEG 4000, 5%(*v*/*v*) 2-propanol, pH 7.3 as a reservoir solution. The crystals were often stuck together and reached final dimensions of 0.1 × 0.1 × 0.3 mm within 2 d (Fig. 2). These crystals diffracted to a maximum resolution of 3.5 Å. A diffraction data set was collected and processed to 3.7 Å resolution (Fig. 3; Table 1). Scaling and inspection of systematic absences revealed that the crystals belonged to the orthorhombic space group $P2_12_12_1$, with unit-cell parameters a = 101.8, b = 115.9, c = 122.8 Å. Calculation of the Matthews coefficient produced a single reasonable solution of 2.68 Å^3 Da^{-1} with one molecule each of EDS1 and SAG101 per unit cell and a corresponding solvent content of 54.14% (Matthews, 1968).

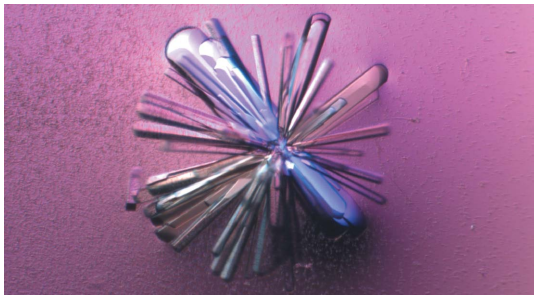

Figure 2
Crystals of the EDS1–SAG101 complex grown using PEG 4000 and 2-propanol as precipitants.

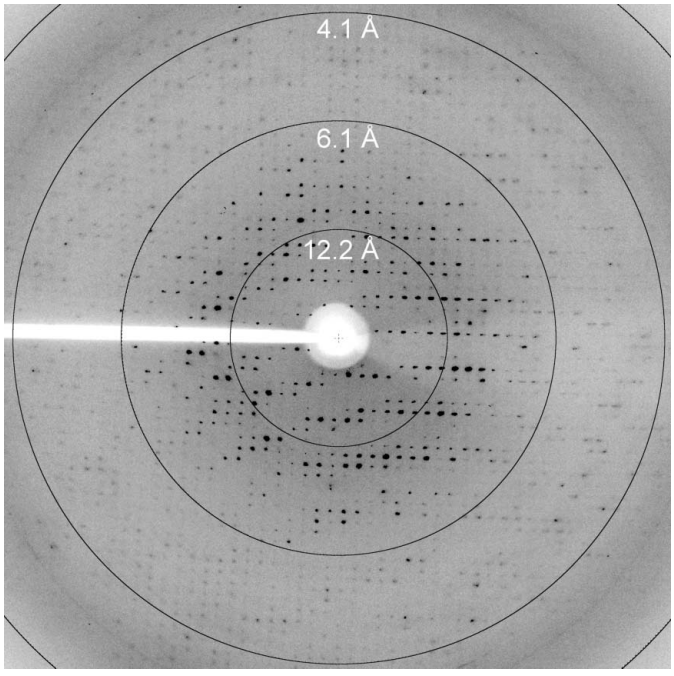

Figure 3
Single X-ray diffraction image of an orthorhombic EDS1–SAG101 crystal showing resolution rings.

Table 1
Typical diffraction data statistics for an EDS1–SAG101 crystal.

Values in parentheses are for the highest resolution shell.

Data-collection wavelength (Å)	0.91841
Resolution range (Å)	35.0–3.73 (3.93–3.73)
Space group	$P2_12_12_1$
Unit-cell parameters (Å)	a = 101.8, b = 115.9, c = 122.8
No. of measured reflections	119759 (13328)
No. of unique reflections	15442 (2076)
Multiplicity	7.8 (6.4)
Unit-cell volume (Å^3)	1.4 × 10^6
Completeness (%)	98.5 (93.4)
$\langle I/\sigma(I)\rangle$	12.0 (3.9)
$R_{\rm merge}$† (%)	11.8 (44.0)

† $R_{\rm merge} = \sum_{hkl}\sum_i |I_i(hkl) - \langle I(hkl)\rangle|/\sum_{hkl}\sum_i I_i(hkl)$.

The overall quality of the data set was low and requires further optimization in order to solve and refine the structure. Although the N-terminal domain of EDS1 and SAG101 is homologous to members of the α/β-hydrolase fold family the sequence identity does not exceed 30%, with the highest similarity being between the N-terminal EDS1 domain and a lipase from *Rhizopus niveus* (PDB code 1lgy; Kohno *et al.*, 1996). Structure determination by the molecular-replacement (MR) method is therefore unlikely to succeed. We have initiated experiments to produce heavy-atom derivatives of the complex for initial phasing. The data presented here provide the first steps towards the ultimate structure determination of this important plant signalling module.

We are grateful to the staff of the BESSY synchrotron, Berlin, Germany for assistance during X-ray diffraction data collection, to Elena Brunstein (Institute of Biochemistry) for excellent technical assistance and to Thomas Colby at the Max Planck Institute for Plant Breeding Research for running the mass spectra. This work was funded by The Max Planck Society and a joint grant (PA 917/3-1; NI 643/2-1) to JEP and KN from the Deutsche Forschungsgemeinschaft.

References

Aarts, N., Metz, M., Holub, E., Staskawicz, B. J., Daniels, M. J. & Parker, J. E. (1998). *Proc. Natl Acad. Sci. USA*, **95**, 10306–10311.
Cheng, Y. T., Germain, H., Wiermer, M., Bi, D., Xu, F., Garcia, A. V., Wirthmueller, L., Despres, C., Parker, J. E., Zhang, Y. & Li, X. (2009). *Plant Cell*, **21**, 2503–2516.
Collaborative Computational Project, Number 4 (1994). *Acta Cryst.* D**50**, 760–763.
Falk, A., Feys, B. J., Frost, L. N., Jones, J. D. G., Daniels, M. J. & Parker, J. E. (1999). *Proc. Natl Acad. Sci. USA*, **96**, 3292–3297.
Feys, B. J., Moisan, L. J., Newman, M. A. & Parker, J. E. (2001). *EMBO J.* **20**, 5400–5411.
Feys, B. J., Wiermer, M., Bhat, R. A., Moisan, L. J., Medina-Escobar, N., Neu, C., Cabral, A. & Parker, J. E. (2005). *Plant Cell*, **17**, 2601–2613.
García, A. V., Blanvillain-Baufumé, S., Huibers, R. P., Wiermer, M., Li, G., Gobbato, E., Rietz, S. & Parker, J. E. (2010). *PLoS Pathog.* **6**, e1000970.
García, A. V. & Parker, J. E. (2010). *Trends Plant Sci.* **14**, 479–787.
He, Y. & Gan, S. (2002). *Plant Cell*, **14**, 805–815.
Jirage, D., Tootle, T. L., Reuber, T. L., Frost, L. N., Feys, B. J., Parker, J. E., Ausubel, F. M. & Glazebrook, J. (1999). *Proc. Natl Acad. Sci. USA*, **96**, 13583–13588.
Kabsch, W. (2010). *Acta Cryst.* D**66**, 125–132.
Kohno, M., Funatsu, J., Mikami, B., Kugimiya, W. & Matsuo, T. (1996). *J. Biochem.* **120**, 505–510.
Mateo, A., Mühlenbock, P., Rustérucci, C., Chang, C. C.-C., Miszalski, Z., Karpinska, B., Parker, J. E., Mullineaux, P. M. & Karpinski, S. (2004). *Plant Physiol.* **136**, 2818–2830.
Matthews, B. W. (1968). *J. Mol. Biol.* **33**, 491–497.

Mühlenbock, P., Szechynska-Hebda, M., Plaszczyca, M., Baudo, M., Mateo, A., Mullineaux, P. M., Parker, J. E., Karpinska, B. & Karpinski, S. (2008). *Plant Cell*, **20**, 2339–2356.
Ollis, D. L., Cheah, E., Cygler, M., Dijkstra, B., Frolow, F., Franken, S. M., Harel, M., Remington, S. J., Silman, I., Schrag, J., Sussman, J., Verschueren, K. H. & Goldman, A. (1992). *Protein Eng.* **5**, 197–211.
Straus, M. R., Rietz, S., Ver Loren van Themaat, E., Bartsch, M. & Parker, J. E. (2010). *Plant J.* **62**, 628–640.
Wiermer, M., Feys, B. J. & Parker, J. E. (2005). *Curr. Opin. Plant Biol.* **8**, 383–389.
Zhou, N., Tootle, T. L., Tsui, F., Klessig, D. F. & Glazebrook, J. (1998). *Plant Cell*, **10**, 1021–1030.